EFFECTS OF LARGE LATE ACCRETION IMPACTS ON EARLY EARTH HABITABILITY.

R. I. Citron[1] and S. T. Stewart[1], [1]Department of Earth and Planetary Sciences, University of California, Davis, CA 95616 (rcitron@ucdavis.edu).

Introduction: Late accretion onto the Hadean Earth included large impacts that could have increased or inhibited early habitability. Sufficiently large impacts could have sterilized the early Earth, with the last sterilizing impact constraining the timing of the emergence of precursors to present-day life [1]. Alternatively, large impacts may have been critical to the emergence of life, delivering iron required to create a reducing environment favorable to the development of RNA precursors [2, 3]. Despite the importance of large (diameter D = 500-3000 km) impacts to early habitability, only limited studies [*e.g.*, 4, 5] have explored the detailed effects of such impacts. Here we present 3D numerical simulations of impacts on the early Earth in order to better quantify the effects of such impacts on planetary habitability. We quantify which impact events would be globally sterilizing and which would deliver sufficient iron to the surface/atmosphere to form a strongly-reducing post-impact environment.

Methods: We modeled 3D impacts by differentiated bodies with 30wt% core onto the early Earth using the Gadget-2 SPH code [6]. We used an updated version of the ANEOS equation of state with new parameters for forsterite and Fe-Si iron alloy to model the planetary mantle and core, respectively [7, 8]. We conducted a set of simulations varying impactor mass (0.0012, 0.003, 0.006, or 0.012 M_{Earth}; D = 1500, 2000, 2700, or 3400 km), impact velocity (1.1, 1.5, or 2 v_{esc}), and impact angle (0, 30, 45, or 60°). An example simulation is shown in Fig. 1.

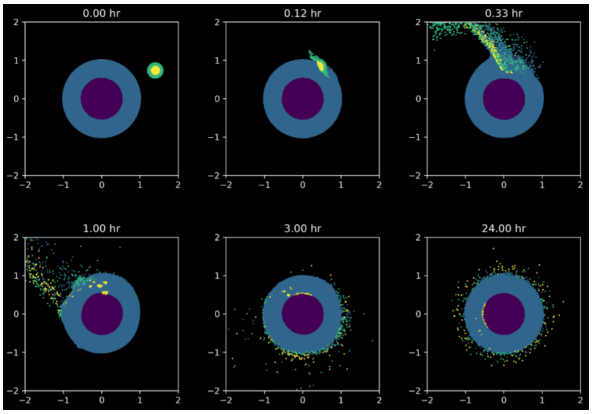

Figure 1: Example simulation of a 0.006 M_{Earth} projectile impact a protoearth target at 1.5 vesc and θ=60°. View of cross section through the equatorial plane with colored dots representing core and mantle particles.

Sterilization: Due to the decrease in impactor size over time, the last sterilizing impact is best constrained by estimating the "minimum sterilizing impact," the smallest scale impact that would make Earth uninhabitable. A lower limit for the minimum sterilizing impact is given by the scale of impact required to vaporize the early ocean via radiation from the hot post-impact rock vapor atmosphere [1]. An upper limit for the minimum sterilizing impact is given by the impact required to globally melt the surface and upper crust [9].

We examine surface melting by determining the equivalent melt depth in the surface layer of SPH particles (Fig. 2). We find that impacts >0.006 M_{Earth} generally deliver sufficient energy to melt most of the surface, while impacts 0.003 M_{Earth} only partially melt (sterilize) the surface. Lower velocity and more grazing impacts also cause less surface melt.

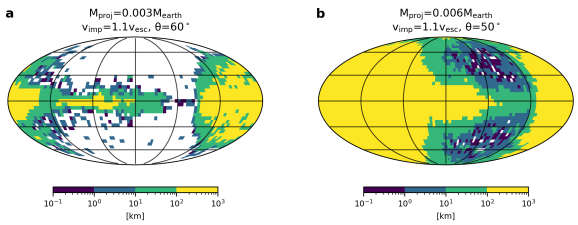

Figure 2: Examples of surface melting for two different simulations. Filled contours correspond to the equivalent melt depth in the outer layer of particles.

We estimate the scale of impact that could vaporize the pre-impact ocean by determining the amount of energy contained in the impact generated hot rock vapor atmosphere. Given that the energy required to vaporize one ocean mass of water (at one bar) is 5×10^{27} J, all of our simulations generated impact vapor with sufficient internal energy to vaporize an ocean mass of water. Extrapolating our results, we find the minimum impact required to vaporize an ocean mass of water is $\sim$ 700 km diameter if impacting at 45° and 16.8 km/s, assuming all of the internal energy increase in the rock vapor is applied towards water vaporization. If half of the energy is radiated outwards into space then an 850 km diameter object would be sufficient.

Iron delivery: The early Earth is expected to have had a weakly-reducing atmosphere, making the generation of a transient strongly-reducing atmosphere via the impact delivery of iron critical to forming an environment favorable for the production of RNA precursor compounds [2, 3]. Late delivery of iron is ex-

pected based on the chondritic proportions of highly siderophile elements (HSEs) in the Earth's mantle [10]. The concentration of HSEs is equivalent to a single impact ($D \sim 3400$ km) of chondritic composition [5, 11].

For each simulation, we quantify the amount of iron deposited into the interior, surface, atmosphere, and ejected from the system after 24 hours of simulation time. The majority of projectile iron is delivered to the mantle, where some proportion may subsequently sink to the core. In general, <20% the projectile iron is delivered to the surface or atmosphere. Iron delivered to the atmosphere would relatively quickly react with pre-impact ocean water that would be in a vapor or supercritical fluid state post-impact. The number of oceans masses of water that could be reduced by the iron deposited in the atmosphere and surface is shown in Fig. 3. This estimate is an upper bound because iron that rains out over molten surfaces may be sequestered at the base of the magma-solid rock interface where it could remain unavailable to react with the steam-rock vapor atmosphere [*e.g.*, 12].

In our simulations, only a few high velocity and high mass impacts at $\theta = 45°$ delivered sufficient iron to the atmosphere to reduce an ocean mass of water, and much of this iron could rain out over a surface that is primarily a magma layer in the aftermath of larger impact events. In general, most impacts $<$ 2700 km diameter deliver insufficient iron to the atmosphere to reduce an ocean mass of water, suggesting that post-impact atmospheres are not as strongly-reducing as previously assumed.

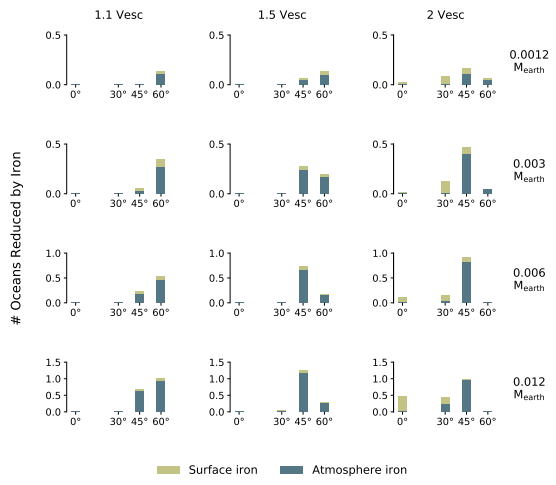

Figure 3: Number of ocean masses that could be reduced from projectile iron delivered in large impacts. Columns and rows correspond to impact velocity and mass, respectively, with bar charts subdivided along the x-axis according to impact angle.

Discussion: Our results suggest that late accretion impacts deliver <20% of the projectile metallic iron to the post-impact rock vapor atmosphere, resulting in less reducing post-impact atmospheres than expected based on the total mass of iron in the impactor. However, interactions between the impact melt and the atmosphere could restore reducing power to the atmosphere [12]. If life did originate in a post-impact environment, its persistence depended on the likelihood of a subsequent sterilizing impact, which we find requires larger projectiles than previously assumed (although several such impacts are expected to have occurred during late accretion). The feasibility of generating RNA precursor chemistry in a post-impact environment relies on a complex balance between requiring an impact sufficiently large to deliver large amounts of reactive iron to the surface, but not so large that subsequent sterilizing events are highly probable.

In ongoing work, we are examining how the inclusion of material strength affects our results. While strength is often neglected in impact models, it can significantly affect model outcomes at these scales [*e.g.*, 13]. Inclusion of material strength results in more localized deposition of the impactor's kinetic energy, which can reduce the overall surface area covered in post-impact melt and increase the size of impact required to globally melt the surface.

Acknowledgements: STS and RIC are supported by Simons Foundation Grant #554203. Modified version of Gadget-2 for planetary impacts is available from the supplement of [14, 15].

References: [1] Sleep N. H. et al. (1989) *Nature*, *342*, 139–142. [2] Benner S. A. et al. (2020) *ChemSystemsChem*, *2*. [3] Zahnle K. J. et al. (2020) *PSJ*, *1*, 11. [4] Svetsov V. V. (2007) *Solar System Research*, *41*, 28–41. [5] Genda H. et al. (2017) *EPSL*, *480*, 25–32. [6] Springel V. (2005) *MNRAS*, *364*, 1105–1134. [7] Stewart S. T. et al., Equation of State Model Forsterite-ANEOS- SLVTv1.0G1: Documentation and Comparisons (2019), *Zenodo*, 10.5281/zenodo.3478631. [8] Stewart S. T., Equation of State Model Fe85Si15-ANEOS: Development and documentation (Version SLVTv0.2G1) (2020), *Zenodo*, 10.5281/zenodo.3866550. [9] Abramov O. and Mojzsis S. J. (2009) *Nature*, *459*, 419–422. [10] Chou C.-L. (1978) *LPSC 9*. [11] Brasser R. et al. (2016) *EPSL*, *455*, 85–93. [12] Itcovitz J. et al. (2021) *EPSC*. [13] Emsenhuber A. et al. (2018) *Icarus*, *301*, 247–257. [14] Ćuk M. and Stewart S. T. (2012) *Science*, *338*, 1047–1052. [15] Carter P., Gadget2-planetary, https://github.com/PhilJCarter/gadget2-planetary (2021), *GitHub*.